Future Foods 4 (2021) 100057

Contents lists available at ScienceDirect

Future Foods

journal homepage: www.elsevier.com/locate/fufo

Effect of thermal and ultrasonic treatments on technological and physicochemical characteristics of fibrous residues from ahipa and cassava starch extraction

K.N. Strack[a], C. Dini[a], M.A. García[a], S.Z. Viña[a,b,*]

[a] CIDCA Centro de Investigación y Desarrollo en Criotecnología de Alimentos, Facultad Ciencias Exactas UNLP – CONICET – CICPBA. 47 y 116 S/N°, La Plata (1900), Buenos Aires, Argentina

[b] Curso Bioquímica y Fitoquímica, Facultad Ciencias Agrarias y Forestales UNLP.

ARTICLE INFO

Keywords:
Manihot esculenta
Pachyrhizus ahipa
Root bagasse
Crude polysaccharides
Residual starch
Autoclaving
Ultrasound
Gelling capacity

ABSTRACT

Fiber-enriched residues from cassava and ahipa roots starch extraction were analyzed by their structural, physicochemical, and techno-functional properties, before and after being subjected to overpressure thermal and ultrasound treatments. Thermal treatment efficiently reduced the residual starch content of both residues (up to 3.4 and 9.6% for ahipa and cassava, respectively), and its combination with ultrasound modified the structural and functional properties of cassava residue, while ahipa bagasse resulted almost unaffected. Ahipa residues swelling power (5.1-5.4 mL/g), WHC (6.9-7.3 g H_2O/g), WBC (4.4-5.4 g H_2O/g), and OBC (3.1-3.3 g oil/g) were in the range reported for several fiber-enriched ingredients, and resulted higher than those of cassava bagasse. Gel-forming capacity was observed for cassava residues coming from starch extraction, mainly due to their residual starch content. This property was lost after thermal treatment, but ultrasound restored the thermally driven gelling capacity. This recovery was associated with fiber structural changes revealed by microscopy, particle size distribution, and FTIR spectra. Based on their gelling properties, thermal and ultrasound-treated cassava bagasse could contribute to modify textural properties in low-calories fruit spreads. Although none of ahipa residues exhibited gelling capacity, their hydration properties and OBC can be applied in the formulation of fiber-enriched bakery products.

1. Introduction

Biomass from food and feed crops provides valuable products, materials, and chemical compounds that can be recovered from waste recycling (Siracusa & Ruberto, 2019). These resources contain high levels of cellulose, hemicellulose, lignin, and in some cases proteins, which can be destined to enhance food products. Presently, dietary fiber (DF) is considered a fundamental part of a healthy diet. Thus, its consumption and use as a food ingredient with specific functions are largely promoted. Soluble and insoluble fiber components show a broad range of technological properties such as water binding, gelling properties, or fat substitution. Additionally, some fiber products are sources of bioactives (Fernandes et al., 2019). This has led to an increase in the availability of marketable food products enriched with DF coming from agricultural by-products (Siracusa & Ruberto, 2019). According to a global forecast (MarketsandMarkets, 2020), the dietary fiber (DF) market is expected to reach USD 9.6 billion by 2025.

Cassava (*Manihot esculenta, Euphorbiaceae*) is a semi-woody shrub that thrives in tropical and subtropical regions, adapted to drought periods and relatively low soil fertility (Saengchan et al., 2015), which makes it a crop of choice in the context of climate change adaptation. Worldwide cassava production involved ~303.6 million tons in 2019 (FAOSTAT, 2021). Cassava roots can be processed into starch, flour, pellets, and chips which are, in turn, inputs for the manufacture of food, bioethanol, paper, textile products, pharmaceuticals, adhesives, etc. However, it is noteworthy that cassava processing generates ~11.1 kg of residue/100 kg of starch produced, which originates environmental concerns such as undesirable odors and water pollution (Chavadej et al., 2019). According to Bizzuti et al., (2021), the by-product from cassava industrial processing (bagasse) shows significant levels of soluble and fibrous carbohydrates which make it, consequently, a potential source of energy in ruminant diets. The authors have reported for this material an appropriate *in vitro* ruminal fermentation performance together with an effective ruminal microbial mass development. Likewise Padi & Chim-

* Corresponding author at: CIDCA Centro de Investigación y Desarrollo en Criotecnología de Alimentos, Facultad de Ciencias Exactas UNLP–CONICET–CICPBA. 47 y 116 S/N°, La Plata (1900), Buenos Aires, Argentina.

E-mail addresses: cdini@biol.unlp.edu.ar (C. Dini), magarcia@quimica.unlp.edu.ar (M.A. García), soniavia@quimica.unlp.edu.ar (S.Z. Viña).

https://doi.org/10.1016/j.fufo.2021.100057
Received 23 February 2021; Received in revised form 4 June 2021; Accepted 13 June 2021
2666-8335/Published by Elsevier B.V. This is an open access article under the CC BY-NC-ND license (http://creativecommons.org/licenses/by-nc-nd/4.0/)

phango (2021), have stated that the transformation of cassava bagasse into high-value bioenergy sources (i.e. bioethanol and bioelectricity) is advantageous both from an economic and environmental point of view.

Ahipa (*Pachyrhizus ahipa* (Wedd.) Parodi) roots stand out as an alternative source of starch, with similar properties to that of cassava (Díaz et al., 2016). The genus *Pachyrhizus* (from the *Fabaceae* botanical family) is native to Southern and Central America. *P. ahipa* has been grown in the pockets of the Andean mountains of Bolivia and Peru, in the fertile valley floors at 1500–3000 m. Along with other Andean crops, ahipa can significantly contribute to diet diversification, increased food security in rural communities, and diminution of monoculture environmental risks (Choquechambi et al., 2019).

Ahipa roots are much more fibrous than cassava, and despite them being rich in starch (54-65% w/w on a dry basis –db-) (Dini et al., 2013) they bear a considerably lower content of this carbohydrate compared to cassava roots (87-91% db) (Saengchan et al., 2015). Thus, ahipa starch extraction at laboratory scale generates about 100 times the wastes produced by the industrial processing of cassava roots (≈1.09 kg of residue/kg of starch, db). Anticipating a potential use of these lignocellulosic residues could help to avoid environmental issues when considering the explotation of ahipa roots at large scale.

According to Nagy et al., (2021), physical, chemical, and biological methods, as well as their combinations, can be used to modify polysaccharides properties such as solubility, swelling, water and oil binding capacity, and/or digestibility, among others, being physical methods generally faster and safer than chemical treatments.

The objective of the present work was to study the main structural, physicochemical, and techno-functional properties of crude polysaccharides that compose the residues of ahipa and cassava starch extraction. The modifications induced by clean, low-cost, and food-compatible methods (autoclaving and ultrasonic treatment) were also analysed.

2. Materials and methods

2.1. Plant materials and fibrous residues

Cassava (Pombero cultivar) and ahipa (IRNAS 9 accession) were grown at Paraje Esperanza (Misiones, Argentina). Roots were washed, sanitized in NaClO solution (250 ppm active chlorine, 10 min), hand-peeled, and cut. Starch was extracted according to Díaz et al., (2016). After six aqueous extractions, a fraction of the insoluble fibrous residue was separated (A1 and C1 for ahipa and cassava, respectively). The remaining residues were resuspended in distilled water (1:1, w:v) and thermally treated in autoclave (121°C, 15 min, 1 atm of overpressure). Insoluble residues were recovered and a portion was separated, filtered and washed with distilled water (1:2, w:v) (residues A2 and C2). Finally, the remaining bagasse was ultrasound-treated (20 kHz, 750 W, 80% amplitude) using a Vibra-Cell™ VCX-750 Ultrasonic Liquid Processor (Sonics & Materials Inc., Newtown, USA) with a CV33 probe. Three 1 min-pulses were applied on the dispersions, which were contained on an ice bath during the treatment. Residues (A3 and C3) were then filtered and washed with distilled water (1:2, w:v). Samples were vacuum-dried at 70°C and 50 mbar (Vacuubrand oven PC 500 Series CVC 3000, Germany) for 48 h, then milled and stored sealed.

2.2. Microscopic analysis

Fibrous residues were observed and photographed with a USB Digital Microscope (Nisuta, Model NS-DIMI, China) and by scanning electron microscopy (SEM). Samples were Au-metallized by sputtering in an SCD030 Balzers equipment and analyzed using a 505 Scanning Electron Microscope (Philips, Eindhoven, the Netherlands), at an accelerating voltage of 20 kV. Images were taken using the Apollo X model EDAX Apex 2 analyzing software.

2.3. Color measurement

A CR-400 colorimeter (Konica Minolta Sensing Inc., Osaka, Japan), calibrated with a standard white plate, was used. L*, a* and b* coordinates were registered. Five repetitions were made for each residue. Results were expressed as total color difference: $\Delta E = \sqrt{\Delta L*^2 + \Delta a*^2 + \Delta b*^2}$

Where ΔL*, Δa* and Δb* are the differences between the coordinate values for the samples and those for the calibration plate. Browning index (BI) was calculated according to Buera et al., (1986).

2.4. Hydration properties

Moisture content (% w/w) was determined gravimetrically by drying at 105°C. Bulk density (BD) and hydration properties were analyzed according to Rosell et al., (2009). BD was calculated as:

BD (g/mL) = dry sample weight (g)/dry sample volume (mL)

For swelling power (SP) measurement, 1 g of residue was accurately weighed in a 15 mL graduated centrifuge tube and sample volume was registered (±0.5 mL). Deionized water was added (1:10 w:v), homogenized and incubated 20 h at 20°C. The volume of the hydrated samples was measured, and SP was calculated as:

SP (mL/g) = [hydrated sample volume (mL) – dry sample volume (mL)]/ dry sample weight (g)

Excess water from the hydrated fibrous residues was removed by aspiration and the tubes were weighed to calculate the water holding capacity (WHC) as:

WHC (g/g) = [wet weight (g) – dry weight (g)]/dry weight (g)

Finally, the tubes were centrifuged (1,500 × *g*, 10 min, room temperature). The non-retained water was discarded, and the pellets were weighed to calculate the water binding capacity (WBC) as:

WBC (w/w) = [weight after centrifugation (g) – dry weight (g)]/dry weight (g)

2.5. Oil Binding Capacity (OBC)

Samples (0.5 g) were accurately weighed in graduated centrifuge tubes and carefully mixed with commercial sunflower oil (1:10, w:v). After 24 h at 20°C, tubes were centrifuged (1,500 × *g*, 10 min). Non-retained oil was discarded, and the pellets were weighed. The OBC was calculated as:

OBC (w/w) = [weight after centrifugation (g) – dry weight (g)]/dry weight (g)

2.6. Remaining starch and phenolic compounds

Starch content (% w/w) was quantified according to Cole et al., (2016). Fibrous residue powders were dispersed in distilled water (1:20, w:v), mixed by vortexing every 10 min for 2 h and filtered. A 10 mL aliquot of a proper dilution of the filtrate was microwave-heated for 1 min and ultrasound-treated using a CV33 probe (450W, 5 min). Samples (800 μL) were added with 0.25M HCl and the iodometric reagent (1mM KIO_3 / 5mM KI), and allowed to rest for 30 min in the dark. Absorbance (λ=600 nm) was measured against an iodometric blank. Calibration curves for ahipa and cassava were obtained using the respective native starche in a concentration range of 50-300 μg/g. Results were expressed as percentage (%, w/w).

Total phenolic compounds (TPC) were quantified spectrophotometrically (λ=760 nm) using the Folin-Ciocalteu reagent (Makkar et al.,

2007). Samples (0.5 g) were extracted with acetone:water (70:30) in an ultrasound bath (2510E-DTH, Branson Ultrasonic Corporation, USA) for 20 min, and then centrifuged (2,000 × *g*, 4°C, 10 min). Supernatants were separated into two fractions: one for the measurement of TPC, and the other for the determination of non-tannin phenolics after treatment with 0.1 g/mL polyvinylpolypyrrolidone (1:1, v:v) (Makkar et al., 2007). The calibration curve was made using gallic acid (0-10 μg/mL). Tannin contents were calculated subtracting non-tannin phenolics from TPC. Results were expressed as mg of gallic acid equivalents/100g of sample.

2.7. Particle size and zeta potential (ζ)

Fibrous residues were passed through an 18-mesh sieve. The retained particles (>1mm) were photographed with a USB Digital Microscope (Section 2.2) and the software ImageJ 1.52a (Java 1.8) was used to determine particle Feret's diameter of at least 180 particles from each sample.

Samples of the non-retained fraction (<1mm) were suspended in distilled water (1:10) and particle size distribution was measured in the range 10-1000 nm using a dynamic light scattering (DLS) particle size analyzer (Malvern Mastersizer 2000E, Malvern Instruments, Worcestershire, UK). The D_{90} (particle size below which 90% of the analyzed particles are found), was registered.

The ζ of aqueous dispersions of the residues (1:100 w/v) was determined at 25°C by DLS using a SZ-100 nanoparticle analyzer (Horiba Ltd.; Kyoto, Japan). After 20 min at room temperature, 1 mL of the suspension was taken from the liquid upper layer and measured. The ζ was reported as the mean of ten readings.

2.8. ATR-FTIR spectra

Samples spectra (at least five for each sample) were collected on a Thermo Nicolet iS10 spectrometer with a diamond ATR accessory (Thermo Scientific, MA, USA), by co-adding 64 scans with 4 cm^{-1} spectral resolution in the range 400-4000 cm^{-1}. The percentage of similarity between the spectra of ahipa and cassava fibrous residues and the respective starch powder was determined in the fingerprint region of sugars (900-1200 cm^{-1}) using the OMNIC software (version 8.3, Thermo Scientific, MA, USA).

2.9. X-ray diffraction analysis

Fibrous residues were analyzed in a Philips PW1830 X-ray diffractometer using Cu K-α radiation and Ni filter. Scans were performed with a step size of 1° and the collection time was 1 min at each step, in the range 2θ=5–70°. Crystallinity degree (CD %) was calculated as the ratio between the absorption peaks area and the diffractogram total area determined using the Origin Pro 8 software (OriginLab®, USA) (Díaz et al., 2018).

2.10. Rheological properties

Cassava residues were dispersed in water (5% w/v) and heated (90°C, 20 min) in a water bath, cooled to room temperature, and analyzed in a RheoStress 600 ThermoHaake (Haake, Germany) rheometer with a plate-plate system PP35 (gap size 1 mm), at 20°C. For rotational tests, samples were allowed to rest for 3 min, then subjected to shear rates from 0 to 500 s^{-1} (3 min), kept at 500 s^{-1} (1 min), and then reduced from 500 to 0 s^{-1} (3 min). Thixotropy (Pa/s) was calculated as the area between the ascendant and descendant flow curves, which were modeled using the Ostwald de Waele equation ($\tau = k\gamma^{\cdot n}$; k: consistency coefficient; n: flow behavior index). Linear viscoelastic region was determined from a stress sweep 0.05-100 Pa. The viscoelastic behavior of thermally treated suspensions was studied by dynamic assays at 1 Pa (within the linear viscoelastic range) according to Díaz et al., (2016). The storage (G') and loss (G") moduli, the tangent of the phase angle (tan δ) and the complex viscosity (η^*) were recorded. Thermally treated suspensions were stored 72 h at 4°C, then equilibrated at 20°C and analyzed by rotational and dynamic modes, as described above. For syneresis analysis, thermally treated suspensions were weighed and stored (72 h, 4°C), then centrifuged (5,000 × *g*, 10 min, 4°C) and weighed again once the supernatants were removed. Syneresis was expressed as percentage (% w/w) of the initial weight.

2.11. Statistical analysis

All determinations were carried out at least in triplicate. Results were subjected to a one-way analysis of variance, followed by a Fisher's Least Significant Difference test, at p=0.05.

3. Results and discussion

3.1. Microscopic analysis and sorption properties

Fig. 1 shows the appearance of cassava and ahipa residues under the stereoscopic microscope. Ahipa residues (Fig. 1 A1-A3) comprised a mixture of clumped and elongated fiber composites with a sawdust appearance, while those from cassava (Fig. 1 C1-C3) seemed mainly as aggregates showing a grainy texture. SEM micrographs (Fig. 2) show ahipa starch granules tucked inside small compartments in A1 fiber structure, but not evidenced in A2 and A3 where these "compartments" seemed broken and turned into grooves along the fibers (Fig. 2 A1-A3). Cassava bagasse C1 was a conglomerate of starchy and fibrous particles (Fig. 2 C1). Small amounts of residual starch were observed in C2 and C3, exhibiting C2 fibrous particles a smoother surface than C3 (Fig. 2 C2-C3).

The main physical properties of ahipa and cassava residues are shown in Table 1. Referring to color, ΔE of A1 fibrous residue was lower ($p<0.05$) than A2 and A3 (Table 1). This was attributed to the reduction of residual starch and the oxidation of the remaining phenolic compounds during the thermal treatment providing darker tones to A2 and A3 (Tables 1 and 2). Similar results were reported by Ullah et al., (2018) for okara insoluble DF which exhibited low whiteness index after being thermally treated in a pressure cooker (120°C for 60 min) and this was attributed to non-enzymatic browning during heating. ΔE of cassava residues was not affected by physical treatments (Table 1). Particularly, among the shades that the incorporation of fiber into food products can provide, brownish tones are valuable for simulating the color that Maillard reactions give during baking, especially to gluten-free bakery products. The browning index (BI) of A1 was significantly higher ($p<0.05$) than that of C1, and they were both increased by the thermal treatment ($p<0.05$) but not by ultrasonication ($p>0.05$), showing A2 and A3 the highest BI values (Table 1).

Bulk density (BD) of ahipa residues (0.3-0.4 g/mL), which showed a "sawdust-appearance" (Fig. 1 A1-A3), was slightly lower than that of cassava residues (0.5-0.7 g/mL), but they were both in the range of other insoluble DF sources such as ginseng (0.58 g/mL) (Hua et al., 2019) or coffee parchment (0.2-0.7 g/ mL) (Benítez et al., 2019).

All samples exhibited moisture contents (Table 1) in the range reported for commercial fibers (Rosell et al., 2009). Residues A1 and C1 showed the highest moisture content, probably related to their high residual starch levels (Table 2). Thermal treatment reduced the moisture content of ahipa and cassava residues while ultrasound did not significantly affect ($p>0.05$) the residual moisture of ahipa residue (A3) but produced a significant decrease in this value for cassava (C3) (Table 1), evidencing a modification of the fiber structure and its interaction with water molecules.

Hydration properties of fiber play a key role in the enhancement of textural and specific technological properties of foods. The swelling power (SP) is related to the potential of fiber as bulking and water retention agent, among other properties. Ahipa samples showed SP values in the range of those reported for commercial oat and bamboo fibers: 4.98 and 5.96 mL/g, respectively (Rosell et al., 2009), but lower than

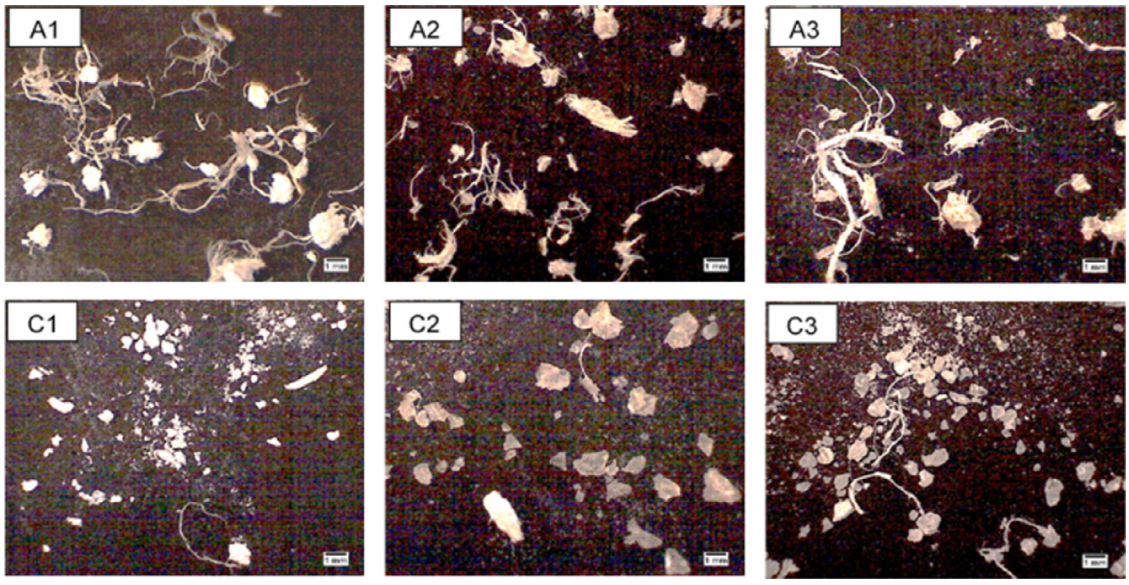

Fig. 1. Root residues observed under digital stereoscopic microscope. A1, A2, A3, C1, C2, C3 correspond to ahipa (A) or cassava (C) fibrous residues obtained after aqueous extractions (1), thermal (2), and thermal+ultrasound (3) treatments.

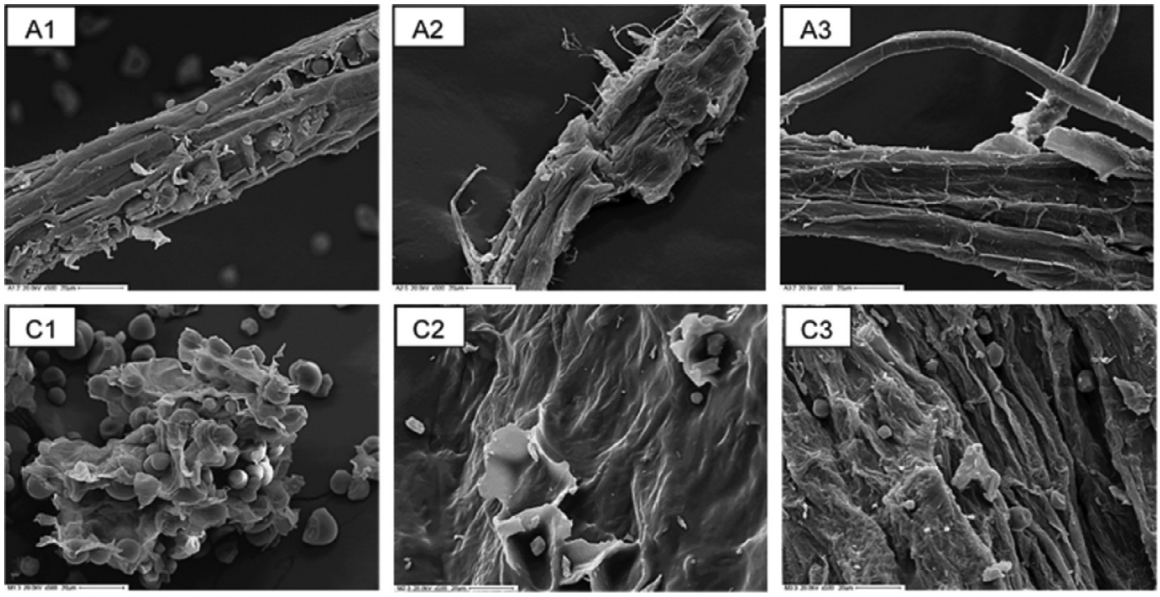

Fig. 2. Scanning electron micrographs of root residues (500 ×). A1, A2, A3, C1, C2, C3 correspond to ahipa (A) or cassava (C) fibrous residues obtained after aqueous extractions (1), thermal (2), and thermal+ultrasound (3) treatments.

Table 1
Physicochemical properties of ahipa and cassava fibrous residues.

Sample	ΔE	BI	Moisture content (%w/w)	SP (mL/g)	WHC (g H_2O/g)	WBC (g H_2O/g)	OBC (g oil/g)
A1	9.14 ± 0.58^{a}	14.7±0.7^{c}	10.86±0.02^{c}	5.4±1.1^{b}	6.94±1.08^{c}	4.43±0.36^{b}	3.26±0.08^{b}
A2	15.99 ± 1.34^{b}	20.7±1.1^{d}	6.81±0.01^{b}	5.1±0.4^{b}	7.34±0.12^{c}	5.42±0.08^{c}	3.20±0.54^{b}
A3	15.92 ± 1.25^{b}	20.2±0.7^{d}	7.52±0.05^{b}	5.4±0.0^{b}	7.08±0.01^{c}	5.27±0.02^{c}	3.08±0.51^{b}
C1	8.35 ± 0.34^{a}	4.6±0.2^{a}	11.95±0.06^{d}	1.7±0.1^{a}	3.08±0.11^{a}	2.25±0.18^{a}	1.71±0.02^{a}
C2	9.17 ± 0.69^{a}	13.7±0.7^{b}	11.00±0.77^{c}	7.0±0.4^{c}	7.88±0.02^{c}	5.64±0.18^{c}	1.31±0.02^{a}
C3	9.35 ± 0.94^{a}	14.5±1.2^{b,c}	5.51±0.18^{a}	4.2±0.0^{b}	5.27±0.00^{b}	4.59±0.01^{b}	1.28±0.11^{a}

Results are expressed as mean±SD in d.b. Different letters within the same column indicate statistically significant differences (p<0.05). ΔE: Total color difference; BI: Browning Index; SP: Swelling Power; WHC: Water Holding Capacity; WBC: Water Binding Capacity; OBC: Oil Binding Capacity. A: ahipa, C: cassava. A1, C1: bagasse from starch extraction; A2, C2: bagasse after thermal treatment; A3, C3: bagasse after thermal and ultrasound treatments.

Table 2
Remaining starch, total phenolics, tannins contents, zeta potential and X-ray diffraction peaks and crystallinity degree of ahipa (A) and cassava (C) fibrous residues.

Sample	Remaining starch (%w/w)	TPC (mg GAE/100 g)	Tannins (mg GAE/100g)	Zeta potential (mV)	2θ of the main peaks (°)	Crystallinity degree (%)
A1	21.94±0.63^{e}	57.1±3.7^{d}	31.6±3.7^{c}	-36.3±5.8^{b}	15; 17; 23	10.69±0.61^{d}
A2	3.42±0.35^{b}	31.8±2.5^{c}	15.8±4.2^{b}	-26.0±2.5^{c}	16; 22.8; 35	11.59±0.44^{e}
A3	2.28±0.13^{a}	21.7±3.3^{b}	14.4±3.4^{a}	-24.4±1.6^{c}	16; 22.8; 35	8.94±0.69^{c}
C1	50.77±0.66^{f}	20.0±0.7^{b}	5.9±5.1^{b}	-65.4±2.5^{a}	15; 17; 23; 35	10.19±0.19^{d}
C2	9.64±0.41^{d}	10.0±1.9^{a}	2.9±2.9^{a}	-14.9±4.5^{d}	20; 35	7.95±0.64^{b}
C3	7.47±0.38^{c}	10.0±0.6^{a}	5.0±0.8^{a}	-14.4±2.6^{d}	16; 20; 35	7.22±0.24^{a}

Results are expressed as mean ± SD in d. b. Different letters within the same column indicate statistically significant differences ($p<0.05$). TPC: total phenolics contents; GAE: gallic acid equivalents; A1, C1: bagasses from starch aqueous extraction; A2, C2: bagasses after thermal treatment; A3, C3: bagasses after thermal and ultrasound treatments.

those of pumpkin enriched fiber products (22.0-41.8 mL/g) (de Escalada Pla et al., 2007). SP of ahipa residues was not modified by the applied treatments. The residue obtained from cassava starch extraction (C1) exhibited a relatively low SP (Table 1), similar to the value reported by Huang Lijie et al. (2018) for a cassava industrial processing residue, and was increased ($p<0.05$) after the thermal treatment (C2), resulting ~4 times that of C1 residue (Table 1) and reaching values in the range of those reported for wheat and oat fibers: 7.1 and 7.6 mL/g respectively (Rosell et al., 2009). Following ultrasonic treatment, SP of C3 residue was reduced up to 60% of that of C2, which might indicate that hydrophobic interactions between fibrous particles were favored after sonication. This would be partially associated with a reduction in particle size, which in turn has been related to lower hydration properties (Rosell et al., 2009).

The WHC and WBC of the samples followed a similar trend to their SP. Ahipa residues did not differ in their WHC, while the WBC was slightly increased after thermal treatment (A2), with no further changes produced by ultrasound. WHC of ahipa was higher than that of bamboo shoot shell fiber (5.9 g/g) (Luo et al., 2017), okara fibers isolated from a sheared suspension (4.9 g/g) (Wang et al., 2019), or lotus node powder (4.3 g/g) (Hussain et al., 2018), but lower than insoluble fiber from ginseng (17.66 g/g) (Hua et al., 2019).

The WHC of the C1 residue was similar to that reported by Huang Lijie et al. (2018) and lower than that of ahipa residue (A1). A significant raise was observed for the WHC and the WBC of cassava residue after thermal treatment (C2) and both parameters were reduced by ultrasonication (C3) (Table 1). Ultrasound produced a modification in the cassava fibrous particles which changed their interaction with water, as reflected by the reduction in their residual moisture and hydration properties. There is limited information about the effect of ultrasound on the physicochemical properties of fiber as food ingredient (Téllez-Morales et al., 2020). In alkali-treated soybean fiber, the application of ultrasound and thermal treatment increased WHC and swelling capacity (Chen et al., 2019). Yan et al., (2020) reported a rise in the WHC and SP of cellulose after ultrasonic treatment. Likewise, ultrasound increased the WBC of insoluble DF from garlic straw (Huang Liuron et al., 2018). However, no consistent trend was observed in the water retention of pulse hulls subjected to ultrasound (Kaya et al., 2017). Fan et al., (2020) found that increasing ultrasound power enhanced the SP and WHC of okara fiber until a limit from which these hydration properties were reduced, probably due to the rupture of pores and channels in the surface of the fibrous particles, which reduced their ability to interact with water molecules. This is in agreement with the smoother surface observed in the present work for C3 particles compared to C2 (Fig. 2 C3).

Regarding the OBC, this property was not affected by the assayed treatments and was rather associated with the bagasse botanical source (Table 1). OBC is an important feature for preventing the loss of oil or fat during food processing and for reducing their absorption during food digestion (Luo et al., 2018). OBC of ahipa residues was approximately twice that of cassava (Table 1), and higher than those reported for lotus node powder (1.6-2.6 g/g) (Chen et al., 2018) and ginseng (1.78 g/g) (Hua et al., 2019), but lower than soybean fiber (5.03 g/g) (Chen et al., 2019) or bamboo shoot shell (5.79 g/g) (Luo et al., 2018). According to Chen et al., (2019), fiber structures that render higher porosity and capillary attraction improve OBC. In this case, ahipa long fibers exhibited surface channels that may increase the capillary attraction with oil, compared to the smaller and smoother particles of cassava residue (Fig. 1).

3.2. Residual starch, phenolics, zeta potential, and particle size

Starch content was high for residues obtained directly from aqueous extractions (A1 and C1, Table 2), presenting C1 the highest value ($p<0.05$), as expected from the higher starch content of cassava compared to ahipa roots (Doporto et al., 2014). Thermal treatment efficiently removed most of the starch from both residues (A2 and C2) and the ultrasound further reduced the amount of A3 and C3 remaining starch, although to a lesser extent than autoclaving (Table 2).

The amount of extractable total phenolics (TPC) was higher for ahipa residues than for cassava, according to their higher content in ahipa roots (Malgor et al., 2020). Thermal treatment significantly reduced TPC and tannins in both A2 and C2, while ultrasound produced a further reduction in ahipa residues (A3) but not in cassava, which was already too low. Phenolic-rich residues are valuable in the food industry to be used as antioxidant fiber (Fierascu et al., 2019). The initial TPC of the studied fibrous residues was markedly lower than the values reported for other plant by-products (Das et al., 2020). However, the antioxidant potential of fibrous residues also relays on non-extractable polyphenols such as polymeric proanthocyanidins and high molecular weight tannins (Sánchez-Alonso et al., 2007). Ahipa residues might present antioxidant potential, especially because they darkened after ~2 months of storage (data not shown), probably associated to the oxidation of remaining polyphenols.

Zeta potential (ζ) of residues aqueous suspensions are shown in Table 2. Higher ζ absolute values were related to higher remaining starch content, representing A1 and C1 the more relatively stable systems amongst the analyzed ones, with higher electrostatic repulsion among particles that could prevent aggregation. Thermal treatment significantly diminished ζ for both ahipa and cassava residues, while ultrasound did not render further modifications. Residues C2 and C3 had the lowest ζ, similar to those reported by de Oliveira et al., (2017) for hydrogels prepared with cellulose fibers extracted from oat and rice husks (-12.5 and -14 mV, respectively). These results indicate that particle surface charge was not directly related to the changes in the hydration properties of cassava residues after ultrasonic treatment.

Fig. 3 shows the effect of the assayed treatments in the particle size distribution of ahipa and cassava residues. As exhibited in Fig. 1, A1 had a high proportion of elongated fibers, being particles >1mm more than 30% in weight (Table inserted in Fig. 3). Within the group of particles <1mm, the proportion of large particles was increased for A2 which was related to the loss of starch granules after thermal treatment (Table 2)

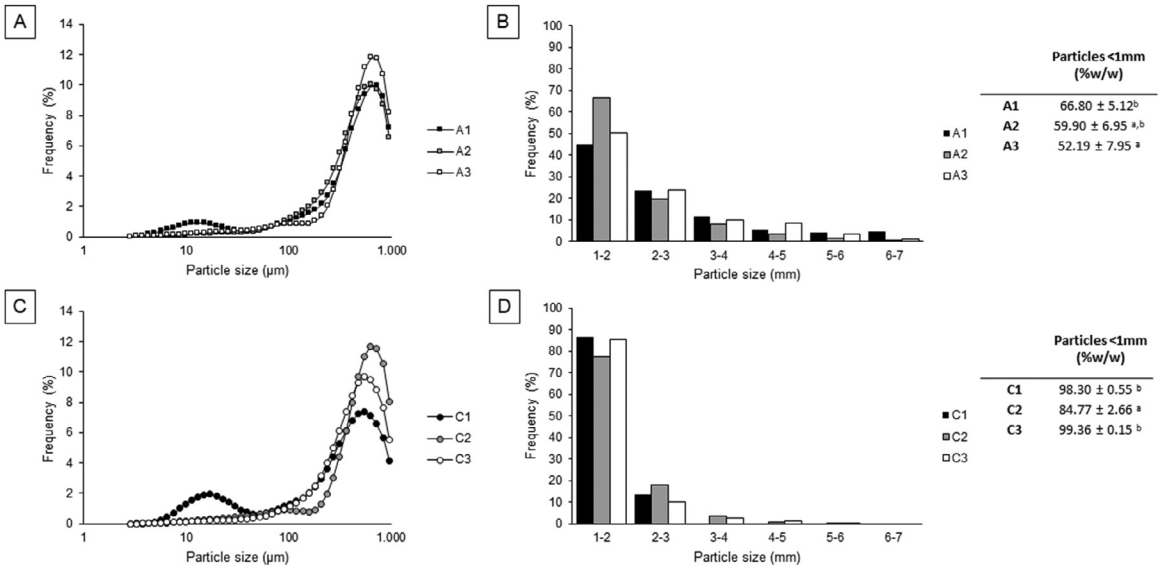

Fig. 3. Size particle distribution of ahipa (A) and cassava (C) residues.

and reflected in the disappearance of the small band at ~13 μm present in A1 (Fig. 3A). The ultrasound treatment (A3) slightly reduced the number of particles in the range ~100-400 μm (Fig. 3A) but this was not reflected in a significant change ($p>0.05$) of the D_{90} value of A2 (552±54 μm) compared to A3 (584±74 μm). However, when analyzing the distribution of particles >1mm, the frequency of particles between 1-2 mm was higher in A2 than in A3, while A3 showed higher proportion of particles >2 mm, indicating that ultrasound did not break the elongated fibers (Fig. 3). The proportion of large (>1mm) to small (<1mm) particles was higher for A3 compared to A1 ($p<0.05$), thus ultrasound treatment did not break large particles but reduced the number of small ones (Table inserted in Fig. 3).

The proportion of particles <1mm was higher in cassava than in ahipa residues for all the assayed treatments (Table inserted in Fig. 3), in agreement to that observed by optical and electron microscopy (Fig. 1 and 2). The proportion of small (<1mm) to large (>1mm) particles was reduced for C2 compared to C1. As stated for ahipa residues, this was related to a reduction of residual starch, also reflected in the disappearance of the band at ~17 μm in C2. Unlike that observed for ahipa, ultrasound significantly reduced the particle size of C3 resulting in almost all the particles below 1mm (Table inserted in Fig. 3). The distribution below 1 mm was slightly modified in the range ~100-400 μm for C3 compared to C2 (Fig. 3C) but no significant difference ($p>0.05$) was observed in their D_{90} values (569±83 and 529±43 μm for C2 and C3, respectively). Within the fraction of particles >1 mm, the proportion of larger elements (>2 mm) was lower for C3 compared to C2, which also indicates a structure breakdown by ultrasonic treatment (Fig. 3D).

3.3. ATR-FTIR and XRD

Fig. 4 shows the ATR-FTIR spectra of ahipa and cassava fibrous residues. As expected, the high starch content in A1 and C1 was reflected in high similarity between the fibrous residue and the respective native starch spectra in the fingerprint region of sugars (900 to 1200 cm^{-1}): 85.4% for A1 and ahipa starch, and 89.4% for C1 and cassava starch. This similarity was reduced after the thermal treatment to 73.8% and 67.2% for A2 and C2, respectively, in agreement with the reduction in their starch content (Table 2). After thermal treatment, a shoulder was observed at 1012 cm^{-1} in C2 which was not evidenced in C1, and ultrasound increased the intensity of this peak (Fig. 4A) indicating changes in the fiber structure. Similar trend was observed for ahipa residues (Fig. 4B). Furthermore, the small peak at ~1103 cm^{-1} in A1, A2, C1, and C2, associated with crystalline cellulose (Martín et al., 2017), was absent in A3 and C3 (Fig. 4).

The characteristic peaks of syringyl (~1325 cm^{-1}) and guaiacyl (~1259 cm^{-1}) units of lignin (Dai & Fan, 2011) or the characteristic lignin bands at 1462 and 1505 cm^{-1} (Pandey & Pitman, 2003) observed for lignin from ahipa and cassava roots (Supplementary Fig. 1) were not evidenced in either of the samples, indicating the predominance of the cellulose and hemicellulose fractions.

Spectra modification by the thermal and ultrasound treatments outside sugars fingerprint region was more pronounced for cassava than for ahipa residues, in agreement with that observed for the physical properties. The peak at 3250 cm^{-1} in C1 and C2, related to OH stretching, was shifted to 3310 cm^{-1} in C3, indicating increased H bonding between the hydroxyl and carboxyl groups in the structure, due to an increment in the number of carboxyl groups (Rashid et al., 2016) evidenced by the intensification of the C=O stretching band at 1735 cm^{-1} in C3 compared to C1 and C2 (Fig. 4B). According to Rashid et al., (2016), this would indicate a reduction in the number of water molecules interacting with the fibrous structure, which is consistent with the lower moisture content of C3 compared to C1 and C2 (Table 1).

For ahipa residues, the change in the -OH stretching band by the thermal and ultrasound treatments was slighter and no changes were evidenced in the carboxyl band at 1735 cm^{-1} (Fig. 4A).

The X-ray diffraction patterns of A1 and C1 resembled those typical of starch, with peaks at 2θ=15, 17, and 23°, reflecting this is the main component in these samples (Table 2). C1 also showed a small peak at 2θ=35° typical of cellulose-containing materials (Chen et al., 2019; Maniglia & Tapia-Blácido, 2019). Crystallinity degrees (CD) of A1 (10.6%) and C1 (10.2%) were similar or slightly lower than the values reported for ahipa and cassava starch (10.6 and 15.9%, respectively) (Díaz et al., 2018; Doporto, 2014), but lower to those reported for insoluble DF from bamboo shoot shell (28.2%, Luo et al., 2018), or ginseng (34.24%, Hua et al., 2019). The CD of C1 was considerably lower than that reported by Huang Lijie et al. (2018) for native cassava residue. However, the authors also reported that crushing the residues decreased the CD in ~17%, thus the low CD observed for cassava residue in the present work might be related to the milling process.

The CD of the ahipa residue was slightly increased after thermal treatment (Table 2) probably due to a counterposed effect between the loss of starch granules (which would decrease the CD) (Maniglia & Tapia-Blácido, 2019) and the removal of amorphous fractions of cellulose and hemicellulose. The ultrasound treatment reduced the CD

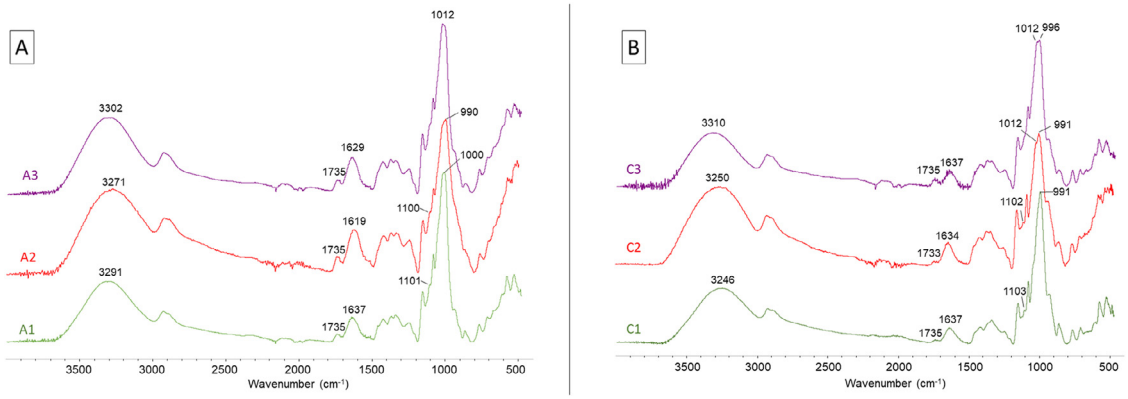

Fig. 4. ATR-FTIR spectra of A) ahipa and B) cassava residues obtained after aqueous extractions (1), thermal (2), and thermal+ultrasound (3) treatments.

Table 3
Rheological parameters from the rotational analysis of cassava residue derived hydrogels.

Sample	Thixotropy (Pa/s)	Ostwald de Waele model			Apparent viscosity η_{ap} (mPa × s)	Syneresis (%w/w)
		r^2	Consistency index k (Pa/s^n)	n		
C1	30225±969^b	0.998	6.911±0.149^c	0.509±0.004^{a,b}	356±13^c	0.10±0.03^a
C2	8754±3417^a	0.988	0.761±0.192^a	0.574±0.044^b	54±4^a	-
C3	11270±721^a	0.968	2.917±1.014^b	0.409±0.037^a	81±7^b	41.73±2.91^b

Results are expressed as mean±SD. Different letters in the same column indicate significant differences (p<0.05).

to 8.9% in A3, probably due to a disruption of the cellulose crystalline structure in agreement with that observed by ATR-FTIR. The diffractograms of A2 and A3 residues were similar to those reported by Luo et al., (2018) for insoluble DF from bamboo shoot shell, with peaks at 2θ=16 and 22.8°, corresponding to type I cellulose.

Thermal treatment reduced the CD of cassava residue from 10.2 to 7.9%, mainly related to the loss of starch. Ultrasound produced a further loss of crystallinity, with C3 showing a CD=7.2%. As observed for C1, both C2 and C3 showed a slight peak at 35° (Table 2) corresponding to type I cellulose (Maniglia & Tapia-Blácido, 2019; Chen et al., 2019).

According to de Oliveira et al., (2017), increased cellulose crystallinity leads to enhanced water absorption of hydrogels. This was not observed in ahipa residues for which ultrasound treatment diminished the CD of A3 compared to A2, but this was not reflected in an appreciable modification of their ATR-FTIR spectra or a significant change (p>0.05) in their moisture content, WHC, or WBC. Conversely, the CD of the ultrasound-treated cassava residue was reduced along with the moisture content, WHC, and WBC, and this was reflected in a structural change when comparing the ATR-FTIR spectra of C3 and C2.

3.4. Rheology

Ahipa residues aqueous suspensions (4% w/w) were not able to form gel-like structures even by heating, thus rheological behavior of these samples was not analyzed.

Aqueous suspensions of cassava residues (4% w/w) subjected to the conditions used for the gelatinization of cassava starch pastes: 90°C, 20 min (Doporto et al., 2014) and equilibrated at room temperature, exhibited a pseudoplastic behavior satisfactorily adjusted to the power-law model. The goodness of fit was reduced from C1 to C3 as reflected by the r^2 values (Table 3). The apparent viscosity (η_{ap}) of C1 was mainly due to its high starch content (Tables 2 and 3), resulting only slightly lower than that of cassava starch pastes: ~400 mPa × s (Díaz et al., 2018) and in the range of the η_{ap} informed for rice fiber and wheat bran (418 and 639 mPa × s, respectively) (Yadav et al., 2017). The n values of all the samples were low and similar to those informed for 4% suspensions of cellulosic arabinoxylan fibers (Yadav et al., 2017), indicating a significant viscosity reduction at high shear rates.

The η_{ap} of C2 was the lowest, while the ultrasound treatment increased the η_{ap} and thixotropy of C3 suspensions (Table 3).

In the amplitude sweep, C1 and C3 suspensions showed linear viscoelastic behavior at shear stresses up to 4 Pa, while for C2 the linear viscoelastic region was lower (up to 0.4 Pa) indicating that C2 behaved as a concentrated solution rather than a weak gel. This heat-induced gel-forming capacity observed for C3 but not for C2 might be related to the increase of carboxyl groups detected by FTIR, which might lead to intra- and intermolecular hydrogen bonding modifying the interaction of the fibrous particles with the surrounding water molecules (Rashid et al., 2016).

As stated, the rheological behavior of C1 was mainly driven by its residual starch content. Accordingly, the G' and G" moduli obtained from the frequency sweep assay at 1Hz resulted only slightly higher than those reported for gelatinized cassava starch pastes (4% w/w): 24 and 7 Pa for G' and G", respectively (Doporto et al., 2014). Heated suspensions of C3 residue exhibited G' and G" values higher than C1 in the entire range of frequencies assayed (Fig. 5A). For both samples, G' and G" remained almost parallel, typical of weak gels.

C3 heat-induced gel-forming capacity was not due to its residual starch content since C2 had more residual starch than C3 (Table 2), thus evidencing changes in the fiber's structure exerted by the ultrasonic treatment. Calabrese et al., (2019) reported that weak gels can be obtained by heating aqueous suspensions of oxidized cellulose nanofibrils at 80°C. This was attributed to enhanced interaction between fibers, which increased the amount of entrapped water providing a semi-solid structure. In the present work, smaller particles and the increased oxidation reflected in the increment in carboxyl groups in C3 might be related to this behavior. Furthermore, in the case of oxidized cellulose nanofibers, the gel-like structure obtained by thermal treatment was maintained after cooling but resulted in a metastable system easily disrupted by mechanical perturbation, indicating the prevalence of hydrophobic interactions between fibers (Calabrese et al., 2019). The same was observed for C3 after refrigerated storage, for which the % of syneresis was considerably higher than that of C1 (Table 3). The syneresis %

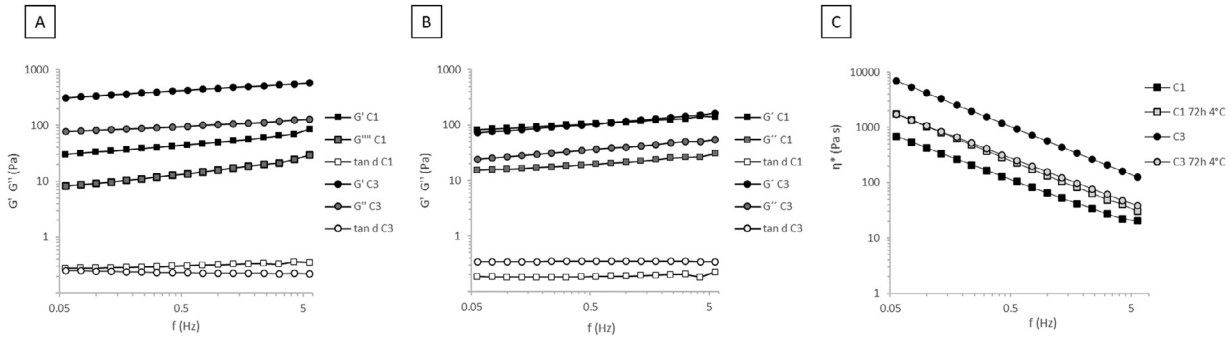

Fig. 5. Storage (G') and loss (G") moduli, and phase angle (tan δ) of the weak gels obtained from 4% w/w aqueous suspensions of C1 and C3 residues heated for 20 min at 90°C A) freshly prepared and B) after refrigerated storage (72h at 4°C). C) Complex viscosity of C1 and C3 gels freshly prepared (black markers) and after refrigerated storage for 72h at 4°C (white markers).

of C1 resulted lower than that reported for gelatinized cassava starch pastes (4.07±0.77%) stored under the same conditions (López, 2011).

The complex viscosity (η^*) of C1 and C3 heated suspensions freshly prepared and after refrigerated storage (72 h, 4°C) are shown in Figure 5C. As observed for both residues hydrogels, the η^* decreased monotonically with the applied frequency. Similar results were reported by Zhang et al., (2014) for cellulose hydrogels from micron-sized bamboo cellulose fibers. Despite C3 exhibited lower η_{ap} than C1 in the rotational assay, the dynamic assay showed an inverse behavior, with C3 showing increased η^* than C1 (Fig. 5C) and higher resistance of freshly prepared C3 suspensions to the dynamic oscillatory share. However, after refrigerated storage, a significant reduction of η^* was observed for C3 hydrogels in the entire range of frequencies assayed, indicating the weakening of the hydrogel structure, while the η^* of C1 was increased, as occurred in pure cassava starch pastes (Supplementary Fig. 2).

4. Conclusion

Thermal treatment under overpressure followed by ultrasound were applied to fibrous residues from cassava and ahipa roots. Added to facilitate starch elimination, treatments modified the structure of the fibrous residues, especially those from cassava, as shown by SEM, FTIR spectra, and X-ray diffraction analysis. Hydration properties of cassava residues (SP, WBC, and WHC) were substantially modified while ahipa residue proved to be less susceptible to structural modifications. Ahipa bagasse showed significantly higher SP, WBC, WHC, OBC, and residual phenolic content than cassava. Only aqueous suspensions of cassava residues C1 and C3 formed weak gels when heated. For C1, this was mainly attributed to the high remaining starch content (~51 % w/w). Thermally treated C2 residue did not form gel structures, but the subsequent ultrasound application allowed to recover weak gelling properties for C3 bagasse, probably due to lower particle size and a slightly higher proportion of carboxyl groups compared to C2, concomitantly with a change in the -OH stretching signal in the FTIR spectra. This indicated increased hydrophobic interactions between fibrous particles which modified the entrapment of the surrounding water during gelling and was also associated with gel disruption after refrigerated storage.

Based on their properties, thermal and ultrasound-treated cassava fibrous residues could contribute to improve textural functionality in products such as low-calorie jams and fruit spreads. According to their color, hydration properties, OBC, and phenolic content, ahipa residues might be used in fiber-enriched bakery products.

Declaration of Competing Interest

The authors of the manuscript entitled “Effect of thermal and ultrasonic treatments on technological and physicochemical characteristics of fibrous residues from ahipa and cassava starch extraction” declare no conflict of interest.

Authors:
STRACK, Karen Nataly
DINI, Cecilia
GARCÍA, María Alejandra
VIÑA, Sonia Zulma
Filiation: CIDCA Centro de Investigación y Desarrollo en Criotecnología de Alimentos, Facultad de Ciencias Exactas UNLP – CONICET La Plata – CICPBA. 47 y 116 S/N°, La Plata (1900), Buenos Aires, Argentina.

La Plata (Buenos Aires, Argentina), 12 January 2021

Acknowledgments

This work was supported by the ANPCyT (PICT-2015-0921 and PICT-2015-3249) and CONICET (PIP-0555 2013-2015) grants. Authors acknowledge F. Versino for providing lignin samples and D. Cabezas for his assistance with the particle size analyzer.

Supplementary materials

Supplementary material associated with this article can be found, in the online version, at doi:10.1016/j.fufo.2021.100057.

References

Benítez, V., Rebollo-Hernanz, M., Hernanz, S., Chantres, S., Aguilera, Y., Martin-Cabrejas, M.A., 2019. Coffee parchment as a new dietary fiber ingredient: Functional and physiological characterization. Food Res. Int. 122, 105–113. doi:10.1016/j.foodres.2019.04.002.

Bizzuti, B.E., de Abreu Faria, L., da Costa, W.S., Lima, P.D.M.T., Ovani, V.S., Krüger, A.M., Louvandini, H., Abdalla, A.L., 2021. Potential use of cassava by-product as ruminant feed. Trop. Anim. Health Prod. 53 (1), 108. doi:10.1007/s11250-021-02555-z.

Buera, M.P., Petriella, C., Lozano, R.D., 1986. Definition of colour in the non-enzymatic browning. Die Farbe 33, 316–326.

Calabrese, V., Muñoz-García, J.C., Schmitt, J., Da Silva, M.A., Scott, J.L., Angulo, J., Khimyak, Y.Z., Edler, K.J., 2019. Understanding heat driven gelation of anionic cellulose nanofibrils: Combining saturation transfer difference (STD) NMR, small angle X-ray scattering (SAXS) and rheology. J. Colloid Interface Sci. 535, 205–213. doi:10.1016/j.jcis.2018.09.085.

Chavadej, S., Wangmor, T., Maitriwong, K., Chaichirawiwat, P., Rangsunvigit, P., Intanoo, P., 2019. Separate production of hydrogen and methane from cassava wastewater with added cassava residue under a thermophilic temperature in relation to digestibility. J. Biotechnol. 291, 61–71. doi:10.1016/j.jbiotec.2018.11.015.

Chen, B., Cai, Y., Liu, T., Huang, L., Deng, X., Zhao, Q., Zhao, M., 2019. Improvements in physicochemical and emulsifying properties of insoluble soybean fiber by physical-chemical treatments. Food Hydrocolloids. 93, 167–175. doi:10.1016/j.foodhyd.2019.01.058.

Chen, H., Zhao, C., Li, J., Hussain, S., Yan, S., Wang, Q., 2018. Effects of extrusion on structural and physicochemical properties of soluble dietary fiber from nodes of lotus root. LWT Food Sci. Technol. 93, 204–211. doi:10.1016/j.lwt.2018.03.004.

Choquechambi, L.A., Callisaya, I.R., Ramos, A., Bosque, H., Mújica, A., Jacobsen, S.E., Sørensen, M., Leidi, E.O., 2019. Assessing the nutritional value of root and tuber crops from Bolivia and Peru. Foods 8 (11), 526. doi:10.3390/foods8110526.

Cole, M.R., Eggleston, G., Gilbert, A., Chung, Y.J., 2016. Development of an analytical method to measure insoluble and soluble starch in sugarcane and sweet sorghum products. Food Chem. 190, 50–59. doi:10.1016/j.foodchem.2015.05.049.

Dai, D., Fan, M., 2011. Investigation of the dislocation of natural fibres by Fourier-transform infrared spectroscopy. Vib. Spectrosc. 55, 300–306. doi:10.1016/j.vibspec.2010.12.009.

Das, A. K., Nanda, P. K., Madane, P., Biswas, S., Das, A., Zhang, W., & Lorenzo, J. M. (2020). A comprehensive review on antioxidant dietary fibre enriched meat-based functional foods. *Trends in Food Science & Technology,* 99, 323–336. https://doi.org/10.1016/j.tifs.2020.03.010.

De Escalada Pla, M. F., Ponce, N.M., Stortz, C.A., Gerschenson, L.N., & Rojas, A.M. (2007). Composition and functional properties of enriched fiber products obtained from pumpkin (*Cucurbita moschata* Duchesne ex Poiret). *LWT Food Science and Technology,* 40, 1176–1185. https://doi.org/10.1016/j.lwt.2006.08.006.

De Oliveira, J.P., Bruni, G.P., Lima, K.O., El Halal, S.L.M., da Rosa, G.S., Dias, A.R.G., da Rosa Zavareze, E., 2017. Cellulose fibers extracted from rice and oat husks and their application in hydrogel. Food Chem. 221, 153–160. doi:10.1016/j.foodchem.2016.10.048.

Díaz, A., Dini, C., Viña, S.Z., García, M.A., 2016. Starch extraction process coupled to protein recovery from leguminous tuberous roots (*Pachyrhizus ahipa*).. Carbohydr. Polym. 152, 231–240. doi:10.1016/j.carbpol.2016.07.004.

Díaz, A., Dini, C., Viña, S.Z., García, M.A., 2018. Technological properties of sour cassava starches: Effect of fermentation and drying processes. LWT Food Sci. Technol. 93, 116–123. doi:10.1016/j.lwt.2018.03.029.

Doporto, M.C., 2014. Doctoral Thesis “Aprovechamiento integral de raíces de ahipa (*Pachyrhizus ahipa*) y sus productos derivados con fines alimentarios. Universidad Nacional de La Plata http://sedici.unlp.edu.ar/handle/10915/34924?show=full.

Doporto, M.C., Dini, C., Viña, S.Z., García, M.A., 2014. *Pachyrhizus ahipa* roots and starches: Composition and functional properties related to their food uses. Starch/Stärke 66, 539–548. doi:10.1002/star.201300196.

Fan, X., Chang, H., Lin, Y., Zhao, X., Zhang, A., Li, S., Feng, Z., Chen, X., 2020. Effects of ultrasound-assisted enzyme hydrolysis on the microstructure and physicochemical properties of okara fibers. Ultrason. Sonochem. 69, 105247. doi:10.1016/j.ultsonch.2020.105247.

FAOSTAT, 2021. Statistics Division. Food and Agriculture Organization of the United Nations http://www.fao.org/faostat/en/#data/QC/Accessed 3 January 2021.

Fernandes, S.S., Coelho, M.S., Salas-Mellado, M.M., 2019. Bioactive compounds as ingredients of functional foods: Polyphenols, carotenoids, peptides from animal and plant sources new. In: Segura Campos, M.R. (Ed.), Bioactive Compounds. Woodhead Publishing, pp. 129–142.

Fierascu, R.C., Fierascu, I., Avramescu, S.M., Sieniawska, E., 2019. Recovery of natural antioxidants from agro-industrial side streams through advanced extraction techniques. Molecules 24 (23), 4212. doi:10.3390/molecules24234212.

Hua, M., Lu, J., Qu, D., Liu, C., Zhang, L., Li, S., Chen, J., Sun, Y., 2019. Structure, physicochemical properties and adsorption function of insoluble dietary fiber from ginseng residue: A potential functional ingredient. Food Chem. 286, 522–529. doi:10.1016/j.foodchem.2019.01.114.

Huang, L., Ding, X., Zhao, Y., Li, Y., Ma, H., 2018. Modification of insoluble dietary fiber from garlic straw with ultrasonic treatment. J. Food Process. Preserv. 42 (1), e13399. doi:10.1111/jfpp.13399.

Huang, L., Zhang, X., Xu, M., An, S., Li, C., Huang, C., Chai, K., Wang, S., Liu, Y., 2018. Dietary fibres from cassava residue: Physicochemical and enzymatic improvement, structure and physical properties. AIP Advances 8, 105035. doi:10.1063/1.5054639.

Hussain, S., Li, J., Jin, W., Yan, S., Wang, Q., 2018. Effect of micronisation on dietary fibre content and hydration properties of lotus node powder fractions. International Journal of Food Science & Technology 53 (3), 590–598. doi:10.1111/ijfs.13632.

Kaya, E., Tuncel, N.B., Tuncel, N.Y., 2017. The effect of ultrasound on some properties of pulse hulls. J. Food Sci. Technol. 54 (9), 2779–2788. doi:10.1007/s13197-017-2714-5.

López, O.V., 2011. Doctoral Thesis “Desarrollo, caracterización y aplicación de envases biodegradables a partir de almidón”. Universidad Nacional de La Plata doi:10.35537/10915/2651.

Luo, X., Wang, Q., Fang, D., Zhuang, W., Chen, C., Jiang, W., Zheng, Y., 2018. Modification of insoluble dietary fibers from bamboo shoot shell: Structural characterization and functional properties. Int. J. Biol. Macromol. 120, 1461–1467. doi:10.1016/j.ijbiomac.2018.09.149.

Luo, X., Wang, Q., Zheng, B., Lin, L., Chen, B., Zheng, Y., Xiao, J., 2017. Hydration properties and binding capacities of dietary fibers from bamboo shoot shell and its hypolipidemic effects in mice. Food Chem. Toxicol. 109, 1003–1009. doi:10.1016/j.fct.2017.02.029.

Makkar, H.P., Siddhuraju, P., Becker, K., 2007. Plant secondary metabolites. In: Walker, JM (Ed.), Methods in Molecular Biology series, 393. Humana Press, USA, pp. 1–122.

Malgor, M., Viña, S.Z., Dini, C., 2020. Root starches enriched with proteins and phenolics from *Pachyrhizus ahipa* roots as gluten-free ingredients for baked goods. International Journal of Food Science & Technology 55 (4), 1763–1772. doi:10.1111/ijfs.14457.

Maniglia, B.C., Tapia-Blácido, D.R., 2019. Structural modification of fiber and starch in turmeric residue by chemical and mechanical treatment for production of biodegradable films. Int. J. Biol. Macromol. 126, 507–516. doi:10.1016/j.ijbiomac.2018.12.206.

MarketsandMarkets, 2020. Dietary fibers market by type (soluble and insoluble), application (functional food & beverages, pharmaceuticals, and feed), source (fruits & vegetables, legumes, cereals & grains, and nuts & seeds), processing treatment, region–Global forecast to 2025 https://www.marketsandmarkets.com/Market-Reports/novel-dietary-fibers-market-858.html.

Martín, C., Wei, M., Xiong, S., Jönsson, L.J., 2017. Enhancing saccharification of cassava stems by starch hydrolysis prior to pretreatment. Ind. Crops Prod. 97, 21–31. doi:10.1016/j.indcrop.2016.11.067.

Nagy, R., Máthé, E., Csapó, J., Sipos, P., 2021. Modifying effects of physical processes on starch and dietary fiber content of foodstuffs. Processes 9, 17 https://doi.org/10.3390/pr9010017.

Padi, R.K., Chimphango, A., 2021. Assessing the potential of integrating cassava residues-based bioenergy into national energy mix using long-range Energy Alternatives Planning systems approach. Renewable Sustainable Energy Rev. 145, 111071. doi:10.1016/j.rser.2021.111071.

Pandey, K.K., Pitman, A.J., 2003. FTIR studies of the changes in wood chemistry following decay by brown-rot and white-rot fungi. Int. Biodeterior. Biodegrad. 52 (3), 151–160. doi:10.1016/S0964-8305(03)00052-0.

Rashid, B., Leman, Z., Jawaid, M., Ghazali, M.J., Ishak, M.R., 2016. Physicochemical and thermal properties of lignocellulosic fiber from sugar palm fibers: Effect of treatment. Cellulose 23 (5), 2905–2916. doi:10.1007/s10570-016-1005-z.

Rosell, C.M., Santos, E., Collar, C., 2009. Physico-chemical properties of commercial fibres from different sources: A comparative approach. Food Res. Int. 42 (1), 176–184. doi:10.1016/j.foodres.2008.10.003.

Saengchan, K., Nopharatana, M., Lerdlattaporn, R., Songkasiri, W., 2015. Enhancement of starch-pulp separation in centrifugal-filtration process: Effects of particle size and variety of cassava root on free starch granule separation. Food Bioprod. Process. 95, 208–217. doi:10.1016/j.fbp.2015.05.008.

Sánchez-Alonso, I., Jiménez-Escrig, A., Saura-Calixto, F., Borderías, A.J., 2007. Effect of grape antioxidant dietary fibre on the prevention of lipid oxidation in minced fish: Evaluation by different methodologies. Food Chem. 101 (1), 372–378. doi:10.1016/j.foodchem.2005.12.058.

Siracusa, L., Ruberto, G., 2019. Not only what is food is good—Polyphenols from edible and nonedible vegetable Waste. In: Watson, R.R. (Ed.), Polyphenols in Plants. Academic Press, pp. 3–21.

Téllez-Morales, J.A., Hernández-Santo, B., Rodríguez-Miranda, J., 2020. Effect of ultrasound on the techno-functional properties of food components/ingredients: A review. Ultrason. Sonochem. 61, 104787. doi:10.1016/j.ultsonch.2019.104787.

Ullah, I., Yin, T., Xiong, S., Huang, Q., Zia-ud-Din, Zhang, J., Javaid, A.B, 2018. Effects of thermal pre-treatment on physicochemical properties of nano-sized okara (soybean residue) insoluble dietary fiber prepared by wet media milling. J. Food Eng. 237, 18–26. doi:10.1016/j.jfoodeng.2018.05.017.

Wang, C., Li, L., Sun, X., Qin, W., Wu, D., Hu, B., Raheem, D., Yang, W., Dong, H., Vasanthan, T., Zhang, Q., 2019. High-speed shearing of soybean flour suspension disintegrates the component cell layers and modifies the hydration properties of okara fibers. LWT Food Sci. Technol. 116, 108505. doi:10.1016/j.lwt.2019.108505.

Yadav, M.P., Kale, M.S., Hicks, K.B., Hanah, K., 2017. Isolation, characterization and the functional properties of cellulosic arabinoxylan fiber isolated from agricultural processing by-products, agricultural residues and energy crops. Food Hydrocolloids. 63, 545–551. doi:10.1016/j.foodhyd.2016.09.022.

Yan, L., Liu, B., Liu, C., Qu, H., Zhang, Z., Luo, J., Zheng, L., 2020. Preparation of cellulose with controlled molecular weight via ultrasonic treatment improves cholesterol-binding capacity. J. Food Process. Preserv. 44 (2), e14340. doi:10.1111/jfpp.14340.

Zhang, X., Wang, Y., Lu, C., Zhang, W., 2014. Cellulose hydrogels prepared from micron-sized bamboo cellulose fibers. Carbohydr. Polym. 114, 166–169. doi:10.1016/j.carbpol.2014.08.012.

Further reading

López, O.V., Versino, F., Villar, M.A., García, M.A., 2015. Agro-industrial residue from starch extraction of *Pachyrhizus ahipa* as filler of thermoplastic corn starch films.. Carbohydr. Polym. 134, 324–332. doi:10.1016/j.carbpol.2015.07.081.

Versino, F., García, M.A., 2014. Cassava (*Manihot esculenta*) starch films reinforced with natural fibrous filler. Ind. Crops Prod. 58, 305–314. doi:10.1016/j.indcrop.2014.04.040.